VOC Sensing Studies on Electrically Conductive Polyaniline@MoS_2 Nanocomposites

RUBY AHMED[1], MOHAMMAD OMAISH ANSARI[2], FARMAN ALI[1] AND SHAHID PERVEZ ANSARI[1*]

[1]Department of Applied Chemistry, Zakir Husain College of Engineering and Technology Aligarh Muslim University, Aligarh-202002
[2]Center of Nanotechnology (CNT), King Abdulaziz University, Jeddah, KSA.

ABSTRACT

Polyaniline (PANI) and molybdenum disulphide (MoS_2) were used to prepare nanocomposites by in-situ oxidative polymerization of acidified aniline in presence of dispersed MoS_2 in the reaction mixture. Electron Microscopy (SEM & TEM), Fourier Transform Infrared (FTIR) spectroscopy, Ultraviolet-Visible (UV-Vis) spectroscopy, and X-ray diffraction (XRD) were used to characterize these nanocomposites. SEM micrographs showed that PANI is present on the layers of MoS_2 which were exfoliated during the preparation and the presence of MoS_2 is also confirmed by XRD peaks. The nanocomposites were studied for their electrical conductivity and stability of electrical conductivity in terms of d.c. electrical conductivity retention. Further, the nanocomposites were also studied for their sensing behaviour towards alcohol, ketone, aldehyde in ambient condition. These nanocomposites were found to be semiconducting, stable upto 100°C and exhibited good sensitivity towards above mentioned group of volatile organic compounds (VOCs).

KEYWORDS: *MoS_2, Nanocomposites, Polyaniline, Sensor, Stability.*

1. INTRODUCTION

Since the discovery of conducting nature of polyaniline (PANI), it has attracted intense attention in diverse field of application. This interest towards the PANI is due to its high electrical conductivity in its emeraldine salt form which may reach to 10^3 to 10^5 Scm^{-1}. [1-7]. Besides its excellent electrical properties, it also exhibits simple redox chemistry i.e. reversible acid/base doping/dedoping process and possesses high stability among other

J. Polym. Mater. Vol. **36,** No. 3, 2019, 243-251

Correspondence author e-mail: shahidzahir@gmail.com
DOI : https://doi.org/10.32381/JPM.2019.36.03.4

conducting polymers. Emeraldine salt is the acid doped conducting form of PANI while emeraldine base is its dedoped and non-conducting form. It is established fact that electrical conductivity of the PANI increases on doping the polymer with acid. The ability to switch between emeraldine salt (conducting) and emeraldine base (non conducting) forms make PANI responsive towards acidic or basic compounds such as ammonia, nitrogen oxides, VOCs etc. The presence of different types of dopants also affects the electrical conductivity of the PANI, therefore, it is considered as promising sensing materials different types of molecules [8-10].

Organic volatile compounds (VOCs) are highly reactive and toxic. These VOCs pose threat to human health by affecting vital organs such as heart, lungs and kidneys, affects fat metabolism and causes respiratory problems. VOCs, specially benzene and alkane derivatives have been associated with lung cancer as they have been found to increase oxygen free radical activity in the cancerous cells [11]. Exposure to CCl_4 is mainly through air and it gets accumulated in body fat and can enter kidney, liver, brain and muscles. High exposure to CCl_4 can cause liver, heart, kidney and nervous system damage. Headache, dizziness and sleepiness are common symptoms of CCl_4 exposure [12]. Inhaling acetone can affect respiratory system, causing irritation in nose and throat and at high concentrations, it can harm the nervous system. Symptoms may include headache, nausea, dizziness, drowsiness and confusion [13]. Methanol is released during industrial vapor, during volcanic eruption, during microbial activities. Exposure of humans to methanol results in blurred vision, dizziness nausea and headache. Ethanol may also be a carcinogenic, studies are still being done to determine this. However, ethanol is a toxic chemical and should be treated and handled with care [14-16].

Molybdenum disulfide (MoS_2) is a two-dimensional, layered structure and has recently attracted high research interest in various important fields of applications due to its excellent optical and electronic properties [17-19]. Besides, MoS_2 nanosheets can be facilely synthesized in large scale and directly dispersed in aqueous solution without the need of surfactants or oxidation treatment. Most recently, PANI was found to effectively improve the conductivity and stability of MoS_2 and has been utilized in designing MoS_2/PANI composites with enhanced electrochemical performances [20-22]. Zhang *et. al.,* [23] prepared PANI/MoS_2 nanocomposite by in-situ hydrothermal process and reported for its electro-catalytic performance on nitrite detection via ampereometery and suggested to be utilized to determine the concentration of nitrites in wide range. Yang and Jiao [24] synthesized thin layered PANI and MoS_2 nanocomposites which exhibited high sensitivity towards chloramphenicol and the electrodes made of these nanocomposites were also found to show greater performance. Li *et al.* [25] suggested higher performance for supercapacitors based on MoS_2/reduced graphene oxide@PANI composite. Hu *et al.* [26] fabricated three dimensional MoS_2/PANI and MoS_2/C for application in lithium ion batteries. Perkin *et al.* [27] reported the chemical vapour sensing by monolayered MoS_2.

With the above considerations, it is believed that PANI@MoS_2 nanocomposites could be utilized for VOC sensing results. And, therefore, in this work we have prepared PANI and PANI@MoS_2 nanocomposites to study the synergistic effect in electrical conductivity, stability and VOCs sensors. Stability of electrical conductivity is of prime importance to any application or study based on conducting materials. Eventually, we have observed increased electrical conductivity, enhanced stability of electrical conductivity and good VOC sensing properties for the PANI@MoS_2 nanocomposites.

2. MATERIALS AND METHOD

2.1 Materials

Aniline (merck, India), molybdenum disulphide (MoS_2) (CDH, India), potassium persulphate (CDH, India), cetyl trimethyl ammonium bromide (CTAB) (CDH, India), HCl (merck, India), ammonia (merck, India) were used as obtained. Double distilled water was used during the process.

2.2 Preparation of PANI@MoS_2 nanocomposites

A series of nanocomposites containing PANI, MoS_2 was prepared (Table 1). In a typical procedure, a reaction mixture containing aniline, CTAB and MoS_2 in 1000ml HCl(1M) was sonicated for 30 min at 4-8 °C. Potassium persulphate (oxidant) was added slowly and the sonication was continued for another 1 hr at the above mentioned temperature. After 1 hr, the reaction mixture was kept in refrigerator for overnight for the reaction to complete. The nanocomposite so obtained was filtered, washed thoroughly with double distilled water and ethanol followed by its dedoping with 1M aqueous ammonia solution. The dedoped nanocomposites were re-doped with 1M HCl, thoroughly washed to eliminate excess of HCl and then dried at 60 °C for 48 hrs in an air oven. Thus prepared PANI@MoS_2 nanocomposites were stored in desiccator for further experiments.

2.3 Characterization:

The nanocomposites of PANI@MoS_2(A1-A5) so prepared were characterized by analytical techniques such as FTIR spectra were obtained by using Perkin-Elmer 1725 instrument. SEM micrographs were obtained by (JEOL, JSM 7600F), XRD analysis was done by (ULTIMA-1V, RIGAKU). PANI and PANI@MoS_2 nanocomposite was tested for DC electrical conductivity measurements and VOCs sensing, the experimental details of which can be seen from our previous reports [10, 21].

TABLE 1. Details of PANI@MoS_2nanocomposites synthesis.

Sample Code	MoS_2	CTAB	Aniline	$K_2S_2O_8$
PANI	0 mole	0.01 mole	0.1 mole	0.05 mole
A1	0.001 mole	0.01 mole	0.1 mole	0.05 mole
A2	0.002 mole	0.01 mole	0.1 mole	0.05 mole
A3	0.003 mole	0.01 mole	0.1 mole	0.05 mole
A4	0.004 mole	0.01 mole	0.1 mole	0.05 mole
A5	0.005 mole	0.01 mole	0.1 mole	0.05 mole

3. RESULT AND DISCUSSION

3.1. Fourier Transform Infrared Spectroscopy (FTIR) Study

FTIR spectra of selected samples, PANI and PANI@MoS_2(A5) nanocomposite are shown in Fig. 1. Peak observed at 3168 cm^{-1} may be

assigned to N-H stretching vibrations of PANI, 1248 cm^{-1} may be attributed to C-N stretching, 808 cm^{-1} may be assigned to out of plane C-H bending vibration of PANI, peaks at 1628 cm^{-1} and 1462 cm^{-1} are due to C=C stretching mode of quinoid and benzenoid rings respectively. In PANI@MoS_2(A5) nanocomposites, the peaks at 1628, 1462 and 1248 cm^{-1} for quinoid ring, benzenoid ring and C-N stretching of PANI respectively are shifted to lower wavelengths in comparison to PANI, thereby indicating a strong interaction between the MoS_2 and PANI matrix.

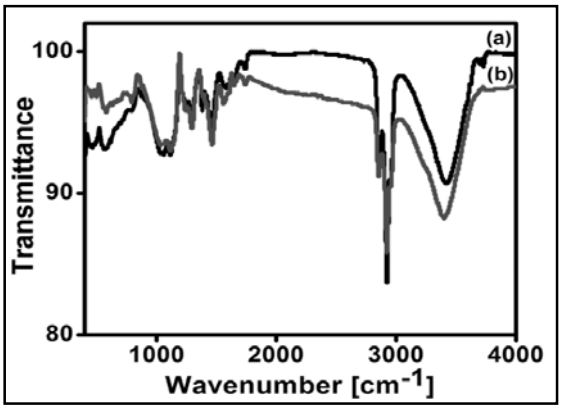

Fig. 1. FTIR spectra of PANI (a) and PANI@MoS_2(b) nanocomposite.

3.2. Scanning Electron Microscopy:

Morphology of PANI and PANI@MoS_2(A5) nanocomposite were studied by electron microscope and are presented in the Fig. 2. It is evident from the Fig. 2a that PANI possesses nano fibrillar morphology and large amounts of fibers are also stacked together at different regions thereby exhibiting flake like structure. The morphology of MoS_2 presented in Fig. 3b shows large sheet like structure with dimension in the range of several hundred nanometers. It is also evident that bulk MoS_2 is agglomerated and layers are not exfoliated. While on the other hand in PANI@MoS_2(A5) nanocomposite, the layers of MoS_2 have been exfoliated and PANI is present within the interlayer space as well as on the surface of MoS_2 (Fig. 2c). It might be interpreted that *in-situ* polymerization process under oxidative conditions resulted in expansion-contraction forces, which simultaneously resulted in exfoliation. Fig. 2 also suggests about the transformation of morphology from flat MoS_2, with increasing percentage of MoS_2. Moreover, porosity is increased by increasing percentage of MoS_2 to core-shell in PANI@MoS_2(A5) nanocomposites. Uniform distribution of MoS_2 and PANI could also be seen.

3.3. Electrical Conductivity Study:

DC electrical conductivity of PANI and PANI@MoS_2 nanocomposites was measured by four-in-line probe method and was found to be in the semiconducting range. The

semiconducting nature of the prepared samples may be seen from the Arrhenius plot (Fig. 3) of the electrical conductivity data. Increase in the electrical conductivity was observed with the increase in the amount of MoS_2 in the nanocomposites. Similar cases are also reported by Ansari et al. for nanocomposites based on PANI and zinc oxide nanoparticles[28-30]. Electrical conductivity of PANI got improved, when loaded with MoS_2 nanoparticles. Improvement in electrical conductivity of PANI when incorporated with MoS_2 nanoparticles was due to formation of efficient network of PANI chains and also due to interaction of PANI with MoS_2, which increased the mobility of charge carriers in PANI@MoS_2 nanocomposites leading to increase in electrical conductivity. Ansari *et. al.,* also reported similar increase in the conductivity of PANI after loading it with TiO_2.[31]

3.4. Stability of Electrical Conductivity in Cyclic Aging Conditions:

In cyclic ageing conditions, the electrical conductivity is measured from room temperature to 100 °C and the experimental setup is allowed to cool down without any disturbance and probe and sample pellet contact was at same position during the course of study. As the sample gets cooled to room temperature, the electrical conductivity was again recorded and this is done for three cycles to assure about the stability of the electrical conductivity. From Fig. (4), it may be seen that the loss in the electrical conductivity is less in PANI@MoS_2 (A5) nanocomposite as compared to the PANI, and therefore, it can be said that the stability of electrical conductivity of PANI@MoS_2 nanocomposites has improved

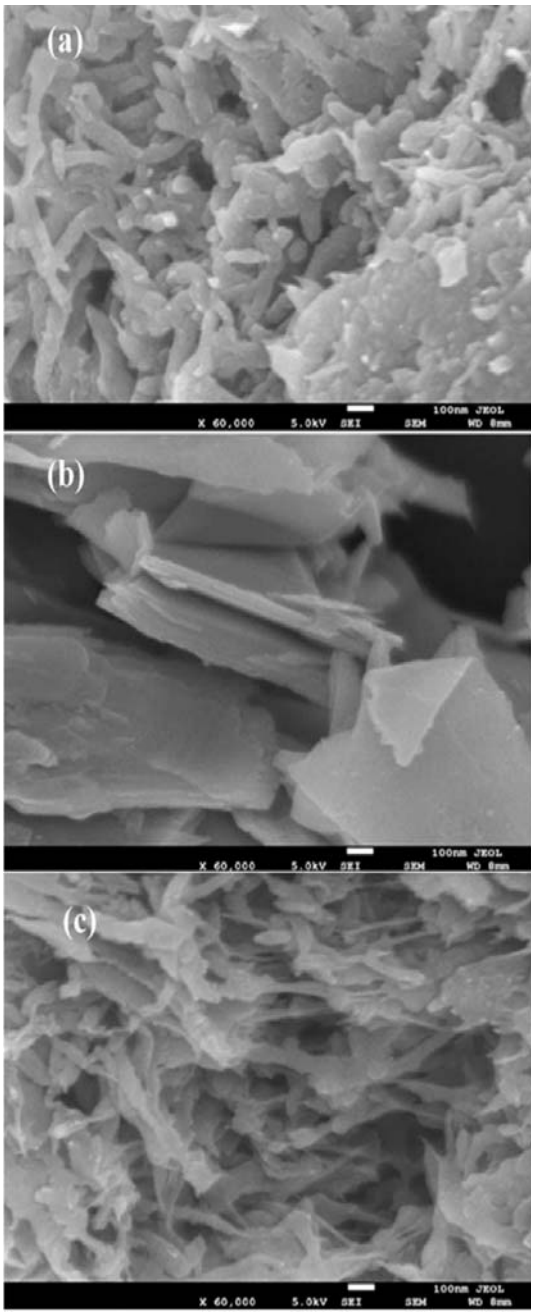

Fig. 2. Scanning Electron Micrographs of (a) PANI, (b) MoS_2 and (c) PANI@MoS_2 (A5) nanocomposite.

and is better than that of PANI [28-31].

3.5 X-ray Diffraction Studies

XRD was done to evaluate the structural characteristics and crystallinity of the PANI, MoS_2, and PANI@MoS_2 nanocomposite (Fig. 5). Fig. 5 shows that PANI is highly amorphous with a characteristic broad peak at ~ 25 2θ due to the periodicity perpendicular to the polymer chain [32]. Pure MoS_2 shows its characteristics peaks at respective 2θ values which matched with the reported literature [33]. For the Pani@MoS_2 nanocomposite, it has a similar XRD pattern to the MoS_2 along with a PANI peak at 25 2θ, confirming the presence of MoS_2 and PANI in the composite. However,

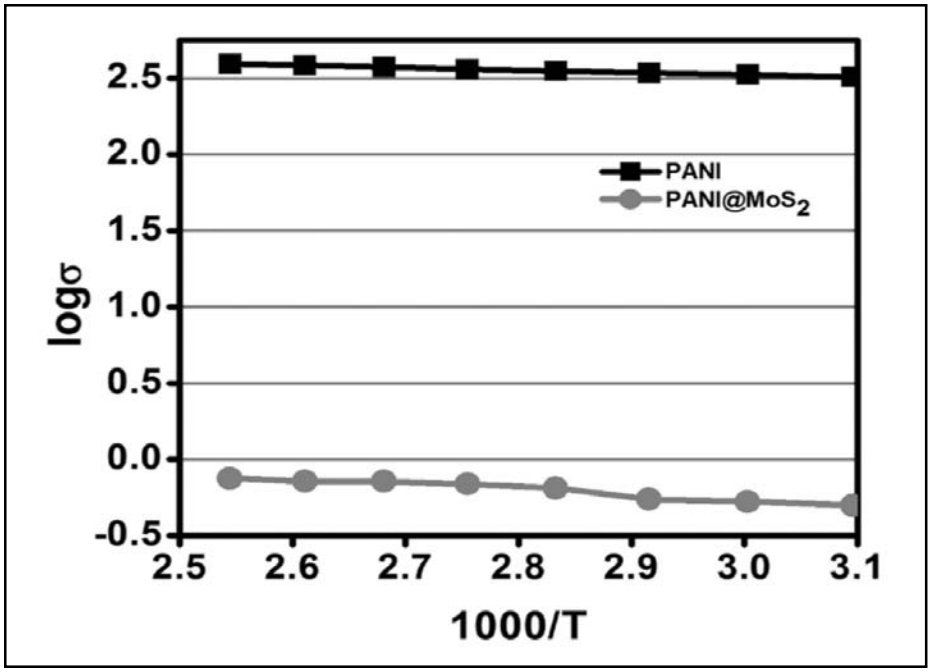

Fig. 4. Arrhenius plot of PANI and PANI@MoS_2.

the peaks of MoS_2 and PANI are slightly diffused and are of much reduced intensity which might be due to the coating of PANI over MOS_2 as well as due to the interaction between amorphous PANI and MoS_2. The existence of the polymer has also been previously reported to influence the degree of crystallization of metal-oxide materials [34].

3.6 VOC Sensing Study:

Sensing of VOCs in our atmosphere and working space is of high importance due to the effects on the human health, directly or indirectly. PANI@MoS_2 nanocomposites was tested for the VOC sensing and compared to PANI. Pure PANI and PANI@MoS_2 was exposed to varour arising from pure samples

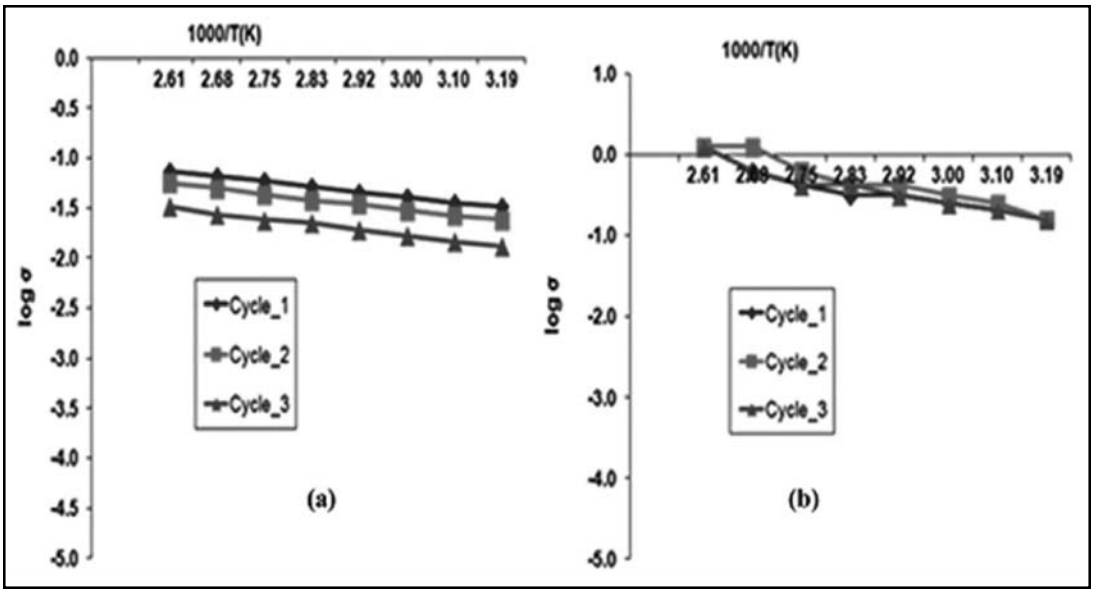

Fig. 5. D.C electrical conductivity stability by cyclic ageing technique of (a) PANI and (b) PANI@MoS_2(A5).

of different VOCs for 30 seconds followed by desorption under normal atmospheric conditions for 30 seconds. Fig. 6. gives an idea of sensing properties of PANI and PANI@MoS_2 nanocomposites. It is clear from the figure that the sensing property of PANI@MoS_2 nanocomposite (A5) sample is better than that of PANI itself. Good signals are seen in different environments (air and medium). It can be seen from the figure that a distinct contrast in the sensing response has been observed for all the VOC's and in general PANI@MoS_2 nanocomposites showed slightly better sensitivity than PANI. This might be due to the increased surface area of PANI@MoS_2 due to the exfoliated MoS_2 as well as surface coating of PANI on MoS_2 and increased conductivity of PANI@MoS_2 due to the better electron transport. The improved sensing properties of as prepared PANI@MoS_2 nanocomposite is believed to be due to the synergetic weak interaction between aromatic aniline and the basal plane of MoS_2 [24]. Perkin el al [27] have suggested that the reason for the improved sensitivity of MoS_2 is its good in-plane conductivity which is derived from sulphur-molybdenum hybridized orbitals and further proposed that the interaction mechanism with the analyte is mediated by the localized lone pair orbitals of the end unit sulphur. Zonnevylle et al. proposed that the orbitals involved in the Mo-S bonds slightly reduce molybdenum and slightly oxidized sulphur and therefore is responsible of creating polarized surface which can interact with a number of analytes with different magnitude. It is believed that further detailed analysis of sensing of wide range of analytes will provide better understanding towards the selectivity and response of these nanocomposites towards any specific analyte [35].

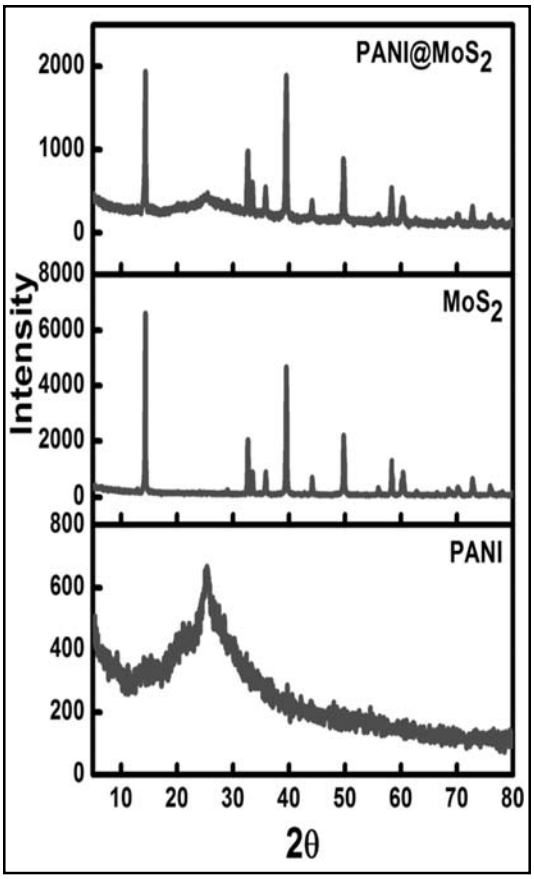

Fig. 5. X-ray diffractogram of PANI, MoS_2 and PANI@MoS_2 nanocomposite.

4. CONCLUSIONS

We have successfully prepared PANI@MoS_2 nanocomposites using bulk MoS_2 by simple route. The SEM studies have shown that the layers of MoS_2 got exfoliated during the preparation of nanocomposites. The as prepared PANI@MoS_2 nanocomposites exhibit higher electrical conductivity and better stability of electrical conductivity as compared to pure PANI. The VOC sensing study showed that the PANI@MoS_2 nanocomposites are better at sensing the various VOCs in ambient conditions. FTIR and XRD data suggest about the interaction of PANI and MoS_2 in the nanocomposites which is believed to be responsible for the higher electrical conductivity, better stability and VOC sensing ability of the PANI@MoS_2 nanocomposites.

REFERENCES

1. G. Cui, J.S. Lee, S.J. Kim, H. Nam, G.S. Cha, H.D. Kim, *Analyst*:123, 1998, 1855-1859.
2. C.G. Wu, T. Bein, *Science* 264, 1994, 1757-1759.
3. N. Ahmad, A.G. MacDiarmid, *Synth. Met.* 85, 1996, 1439-1440.

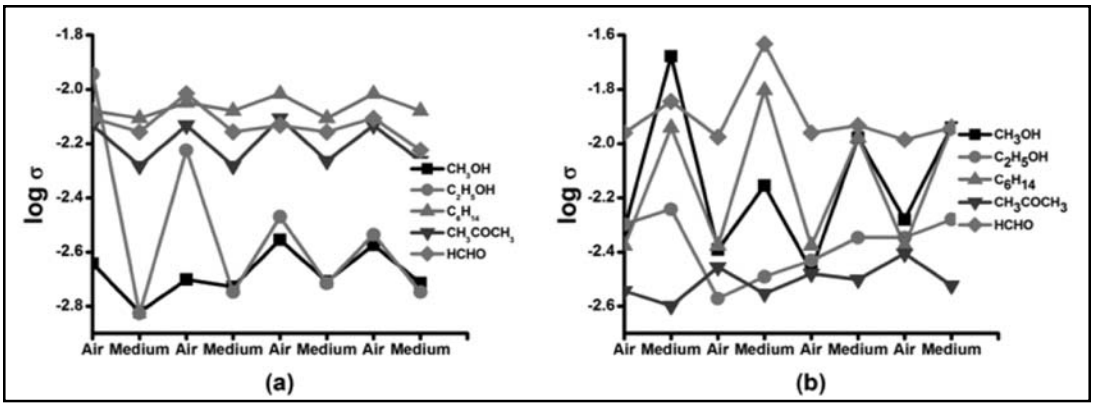

Fig. 6. Chemical Sensing of VOCs by (a) PANI and (b) PANI@MoS_2 nanocomposite.

4. A.G. MacDiarmid, *Synth. Met.* 84, 1996, 27-34.
5. A.A. Khan, M. Khalid, *J. Appl. Polym. Sci.*, 117, 2010, 1601-1607.
6. C.Y. Yang, Y. Cao, P. Smith, A.J. Heegar, *Synth. Met.* 1993, 53, 293-301.
7. Y. Cao, P. Smith, C. Yang, *Synth. Met*. 69, 1995, 191-192.
8. SP Ansari, F. Mohammad, *Polym. and Polym. Comp*., 24, 2016, 273-280.
9. SP Ansari, F. Mohammad, *Iran. Polym. J.*, 25, 2016, 363-371.
10. M.O. Ansari, SP Ansari, SK. Yadav, T. Anwer. MH Cho, F. Mohammad, *J. Ind. Engg. Chem*. 20, 2014, 2010-2017.
11. P. Anil Kumar, M. Jayakannan, *Langmuir*, 2008, 24, 9754-9762
12. F-Y. Yi, S-C. Wang, M. Gu, J-Q. Zheng, L. Han, *J. Mater. Chem. C*, 6, 2018, 2010-2018.
13. D. Dreher, A.F. Junod, *Eur. J. Cancer* 32A ,1916, 30-38.
14. P.A. Sobotka, D.K. Gupta, D.M. Lansky, M.R. Costanzo, E.J. Zarling, *J Heart Lung Transplant* 13, 1994, 224-29.
15. S. Humad, E.J. Zarling, M. Clapper, *Free Rad. Res. Commun.* 5, 1998, 101-106.
16. C.O. Olopade, M. Zakkar, W.I. Swedler, I. Rubinstein, *Chest* 11, 1997, 862-865.
17. T. Zhang, S. Mubeen, B. Yoo, N.V. Myung, M.A. Deshusses. *Nanotech*. 20, 2009, 225509, 1-5.
18. X.B. Yan, Z.H. Han, Y. Yang, B.K. Tay, *Sens. Actuators B* 123, 2007, 107-113.
19. S. Virji, R. Kaner, B. Wellier. *J. Phys. Chem B* 110, 2006, 22266-22270.
20. Y. Xia, X. Lu, H. Zhu, *Natural silk fibroin/ polyaniline (core/shell) coaxial fiber: Fabrication and application for cell proliferation, composite science and technology*, 77, 2013, 37-41.
21. M.O. Ansari, F. Mohammad, *Sens. Actuators B* 157, 2011, 122-129.
22. Y.Y. Xia, Y. Lu, *Polym. Composites*, 31, 2010, 340-346.
23. Y. Zhang, P. Chen, F. Wen, C. Huang, H. Wang, *Ionics* 22, 2016, 1095–1102.
24. T. Yang, K. Jiao, H-Y. Chen, J. Wang, L. Meng, *Chinese Chemical Letters* 27, 2016, 231–234.
25. X. Li, C. Zhang, S. Xin, Z. Yang, Y. Li, D. Zhang, P. Yao, *ACS Appl. Mater. Interfaces*, 8, 2016, 21373–21380.
26. L. Hu, Y. Ren, H. Yang, Q. Xu, *ACS Appl. Mater. Interf.* 6, 2014, 14644–14652.
27. F. K. Perkins, A. L. Friedman, E. Cobas, P. M. Campbell, G. G. Jernigan, B. T. Jonker, *Nano Lett.* 13, 2013, 668–673.
28. SP. Ansari and F. Mohammad, *IUP J. Chem*. 4, 2010, 7-18.
29. S. P. Ansari and F. Mohammad, *ISRN Material Science* 2012, ID 129869, 1-7.
30. S. P. Ansari and F. Mohammad, *SMC bulletin* 9, 2018, 13-19.
31. M.O. Ansari and F. Mohammad, *J. App. Polym. Sci*., 124, 2012, 4433-4442.
32. M. O. Ansari, F. Mohammad, *Compos. B: Eng*, 43, 2012, 3541-3548.
33. X. Wang, Y. P. Zhang, Z. Q. Chen, *Chalcogenide Lett.,* 13, 2016, 351 – 357.
34. X. Zhang, X. Zeng, M. Yang, Y. Qi, *ACS Appl. Mater. Interface*, 6, 2014, 1125-1130.
35. M.C. Zonnevylle, R. Hoffmann, S. Harris, *Surf. Sci.* 199, 1988, 320–360.

Received: 10-07-2019

Accepted: 28-08-2019